1-1-2021

Pattern and degree of individual brain atrophy predicts dementia onset in dominantly inherited Alzheimer's disease

Ophir Keret

Randal J Bateman

Tammie L S Benzinger

John C Morris

Beau M Ances

See next page for additional authors

Authors

Ophir Keret, Randal J Bateman, Tammie L S Benzinger, John C Morris, Beau M Ances, Nelly Joseph-Mathurin, Richard J Perrin, Brian A Gordon, Dominantly Inherited Alzheimer Network, and et al

Received: 6 April 2021 | Accepted: 13 April 2021 | Published online: 24 May 2021

DOI: 10.1002/dad2.12197

Alzheimer's & Dementia
Diagnosis, Assessment & Disease Monitoring

RESEARCH ARTICLE

Pattern and degree of individual brain atrophy predicts dementia onset in dominantly inherited Alzheimer's disease

Ophir Keret[1] | Adam M. Staffaroni[2] | John M. Ringman[3] | Yann Cobigo[2] | Sheng-Yang M. Goh[2] | Amy Wolf[2] | Isabel Elaine Allen[1,4] | Stephen Salloway[5] | Jasmeer Chhatwal[6] | Adam M. Brickman[7] | Dolly Reyes-Dumeyer[7] | Randal J. Bateman[8,9,10,11,12] | Tammie L.S. Benzinger[8,10] | John C. Morris[8,9,10,11,12] | Beau M. Ances[8,9,10,11,12] | Nelly Joseph-Mathurin[8,9,10,11,12] | Richard J. Perrin[8,9,10,11,12] | Brian A. Gordon[8,9,10,11,12] | Johannes Levin[13,14] | Jonathan Vöglein[13,14] | Mathias Jucker[15,16] | Christian la Fougère[15,17] | Ralph N. Martins[18,19,20,21,22] | Hamid R. Sohrabi[18,19,20,21,22] | Kevin Taddei[19,21] | Victor L. Villemagne[23] | Peter R. Schofield[24,25] | William S. Brooks[24,26] | Michael Fulham[27] | Colin L. Masters[28] | Bernardino Ghetti[29] | Andrew J. Saykin[30,31] | Clifford R. Jack[32] | Neill R. Graff-Radford[33] | Michael Weiner[34,35,36,37,38] | David M. Cash[39,40] | Ricardo F. Allegri[41] | Patricio Chrem[41] | Su Yi[42] | Bruce L. Miller[1,2] | Gil D. Rabinovici[1] | Howard J. Rosen[1,2] | Dominantly Inherited Alzheimer Network

[1] Global Brain Health Institute, University of California, San Francisco, California, USA

[2] Department of Neurology, Memory and Aging Center, University of California, San Francisco, California, USA

[3] Alzheimer's Disease Research Center, Keck School of Medicine, University of Southern California, Los Angeles, California, USA

[4] Department of Epidemiology and Biostatistics, University of California, San Francisco, California, USA

[5] Warren Alpert Medical School, Brown University, Providence, Rhode Island, USA

[6] Massachusetts General Hospital, Harvard Medical School Boston, Boston, Massachusetts, USA

[7] Taub Institute for Research on Alzheimer's Disease and the Aging Brain, Columbia University, New York, New York, USA

[8] Charles F. and Joanne Knight Alzheimer Disease Research Center, Department of Neurology, Washington University School of Medicine, St. Louis, Missouri, USA

[9] Department of Neurology, Washington University School of Medicine, St. Louis, Missouri, USA

[10] Department of Radiology, Washington University School of Medicine, St. Louis, Missouri, USA

[11] Division of Neuropathology, Department of Pathology & Immunology, Washington University School of Medicine, St. Louis, Missouri, USA

[12] Division of Biostatistics, Department of Psychiatry, Washington University in St. Louis School of Medicine, St. Louis, Missouri, USA

[13] German Center for Neurodegenerative Diseases (DZNE), Munich, Germany

[14] Department of Neurology, Ludwig-Maximilians-Universität München, Munich, Germany

[15] German Center for Neurodegenerative Diseases (DZNE), Tübingen, Germany

[16] Department of Neurodegenerative Diseases, Hertie Institute for Clinical Brain Research, University of Tübingen, Tübingen, Germany

[17] Institute for Nuclear Medicine and Clinical Molecular Imaging, Eberhard Karls University, Tübingen, Germany

[18] Department of Biomedical Sciences, Macquarie University, North Ryde, New South Wales, Australia

[19] Centre of Excellence for Alzheimer's Disease Research and Care, School of Medical and Health Sciences, Edith Cowan University, Joondalup, Western Australia, Australia

[20] School of Psychiatry and Clinical Neurosciences, University of Western Australia, Crawley, Western Australia, Australia

[21] Australian Alzheimer's Research Foundation, Nedlands, Western Australia, Australia

[22] The Cooperative Research Centre for Mental Health, Carlton South, Victoria, Australia

[23] Department of Molecular Imaging and Therapy, Austin Health, Melbourne, Victoria, Australia

[24] Neuroscience Research Australia, Randwick, Sydney, New South Wales, Australia

[25] School of Medical Sciences, UNSW Sydney, Sydney, New South Wales, Australia

[26] Prince of Wales Hospital Clinical School, UNSW Sydney, Sydney, New South Wales, Australia

[27] Department of Molecular Imaging, Royal Prince Alfred Hospital, Sydney Medical School, University of Sydney, Camperdown, New South Wales, Australia

[28] The Florey Institute, University of Melbourne, Parkville, Victoria, Australia

[29] Department of Pathology and Laboratory Medicine, Indiana University School of Medicine, Indianapolis, Indiana, USA

[30] Department of Neurology, Indiana University School of Medicine, Indianapolis, Indiana, USA

[31] Department of Radiology, Indiana University School of Medicine, Indianapolis, Indiana, USA

[32] Department of Radiology, Mayo Clinic, Rochester, Minnesota, USA

[33] Department of Neurology, Mayo Clinic, Jacksonville, Florida, USA

[34] Department of Veterans Affairs Medical Center, Center for Imaging of Neurodegenerative Diseases, San Francisco, California, USA

[35] Department of Radiology, University of California, San Francisco, San Francisco, California, USA

[36] Department of Medicine, University of California, San Francisco, San Francisco, California, USA

[37] Department of Psychiatry, University of California, San Francisco, San Francisco, California, USA

[38] Department of Neurology, University of California, San Francisco, San Francisco, California, USA

[39] Dementia Research Centre, Department of Neurodegenerative Disease, UCL Queen Square Institute of Neurology, University College London, London, UK

[40] Centre for Medical Image Computing, Department of Medical Physics and Biomedical Engineering, University College London, London, UK

[41] Department of Cognitive Neurology, Neuropsychiatry and Neuropsychology, Instituto de InvestigacionesNeurológicas FLENI, Buenos Aires, Argentina

[42] Banner Alzheimer's Institute, Phoenix, Arizona, USA

Correspondence
Ophir Keret, Global Brain Health Institute, University of California, Zabutinsky 39, Petach Tikva, Israel.
Email: Ophir.keret@gbhi.org

Funding information
National Institutes of Health, Grant/Award Numbers: P01 AG019724, P30 AG062422, K24 AG045333, U19 AG063911, U01 AG045390, U54 NS092089, U01AG051218, P50AG016570, P50AG005142, K08AG022228, P30 AG066444, P01 AG03991, P01 AG026276, U19 AG032438, P30 AG010133, R01 AG019771, P30 AG010133, R01 AG019771, R01 AG057739, U01 AG024904, R01 LM013463, R01 AG068193, U01 AG068057

Abstract

Introduction: Asymptomatic and mildly symptomatic dominantly inherited Alzheimer's disease mutation carriers (DIAD-MC) are ideal candidates for preventative treatment trials aimed at delaying or preventing dementia onset. Brain atrophy is an early feature of DIAD-MC and could help predict risk for dementia during trial enrollment.

Methods: We created a dementia risk score by entering standardized gray-matter volumes from 231 DIAD-MC into a logistic regression to classify participants with and without dementia. The score's predictive utility was assessed using Cox models and receiver operating curves on a separate group of 65 DIAD-MC followed longitudinally.

Results: Our risk score separated asymptomatic versus demented DIAD-MC with 96.4% (standard error = 0.02) and predicted conversion to dementia at next visit (hazard ratio = 1.32, 95% confidence interval [CI: 1.15, 1.49]) and within 2 years (area under the curve = 90.3%, 95% CI [82.3%–98.2%]) and improved prediction beyond established methods based on familial age of onset.

Discussion: Individualized risk scores based on brain atrophy could be useful for establishing enrollment criteria and stratifying DIAD-MC participants for prevention trials.

KEYWORDS
autosomal dominant Alzheimer's disease, brain atrophy, Dominantly Inherited Alzheimer Network, preclinical Alzheimer's disease

1 | INTRODUCTION

Alzheimer's disease (AD) is a devastating progressive neurodegenerative disease with high worldwide prevalence. Recent drug trials for patients with dementia and underlying AD have failed to show meaningful benefit.[1,2] One potential explanation for the failure to demonstrate efficacy is that the interventions were given at disease stages that are too late to alter clinical progression.[3] Many ongoing trials are attempting treatment at an earlier stage, such as at the time of mild cognitive symptoms or before the onset of cognitive symptoms.[4,5] To evaluate the ability of these interventions to prevent development of dementia, researchers need to recruit individuals with a very high risk of developing symptoms of dementia over the duration of a clinical trial (usually 1 or 2 years).[3] Carriers of mutations in genes that cause dominantly inherited AD (DIAD), such as presenilin-1 (*PSEN1*), presenilin-2 (*PSEN2*), and amyloid precursor protein (*APP*), are certain to develop dementia, and thus are ideal candidates for AD prevention studies.

Nearly all DIAD mutation carriers (DIAD-MC) develop dementia. Although the time until the onset of dementia can be estimated based on the age of symptom onset from individuals with the same type of muation,[6] variability of several years is frequently observed, and this can occur even within the same family.[7]

Another approach for approximating time to symptom onset is to use established biological markers of disease (biomarkers). Similar to sporadic AD, DIAD-MC undergo biological changes years before the onset of dementia.[8,9] Such changes can be measured with magnetic resonance imaging (MRI);[6,8,10–17] cerebrospinal fluid (CSF) levels of amyloid beta (Aβ) and phosphorylated tau and total tau;[6,8,12,18] and positron emission tomography (PET) radiotracers that measure glucose metabolism,[6,8,12] Aβ[6,12] fibrils, and tau accumulation.[19] Indeed, previous studies have shown that changes in many of these biomarkers precede cognitive decline in DIAD-MC.[12] Some of the aforementioned imaging modalities are expensive, involve exposure to ionizing radiation, and are relatively scarce in many parts of the world. It is thus encouraging that baseline hippocampal volume and change in hippocampal volume over time, which can be measured from MRI, are both predictive of decline in DIAD-MC.[12] Changes in volume in other brain regions are also predictive of cognitive decline in DIAD-MC.[10,14] This would be expected given that cognition is dependent on many brain regions and that AD characteristically spreads through the brain as disease advances.[20] Prior studies in sporadic AD have indicated that measurements of volume across the brain can predict likelihood of developing dementia.[21,22] Together, these findings suggest that quantification of volume loss across the brain might provide a good predictor of time to onset of dementia. If such an estimate could be derived from a single measurement, it would further improve its value, for instance by allowing people who appear far from dementia to defer follow-up for a longer period compared to those in whom dementia is imminent.

Individualized atrophy-based risk scores have been previously reported to predict symptom onset in asymptomatic carriers of mutations that cause frontotemporal dementia.[23] The risk score uses calculated atrophy in each brain region at a single time point to predict the individual's risk for dementia at subsequent visits. The aim of the current study was to evaluate whether a similar method is useful in DIAD and to assess its added benefit beyond the estimated years to onset (EYO) that is calculated based on the reported age of onset for each specific DIAD mutation.

HIGHLIGHTS

- Brain atrophy precedes cognitive decline by years in dominantly inherited Alzheimer's disease.
- Brain atrophy–based risk scores can predict dementia onset in mutation carriers.
- Risk score can help establish enrollment criteria for Alzheimer's disease prevention trials.

2 | METHODS

2.1 | Overview

Our analysis was conducted in two stages. The first stage used logistic regression in cognitively normal DIAD-MC participants and DIAD-MC patients with established dementia at study entry to identify a pattern of atrophy associated with the presence of dementia and to develop a dementia risk score that can be calculated based on the similarity of a given individual's regional brain volumes to that pattern. In the second stage of the analysis, the risk score was applied to DIAD-MC participants who had not yet developed dementia at study entry and who were followed longitudinally, and the ability of the risk score to predict onset of dementia at follow-up was assessed.

2.2 | Subjects

We included 216 DIAD-MC enrolled in the Dominantly Inherited Alzheimer Network (DIAN; 12th data freeze, 2008 to 2017), and 15 DIAD-MC seen at the Alzheimer's Disease Research Centers at the University of California Los Angeles (ADRC-UCLA) and University of Southern California (ADRC-USC), as well as 99 non-carrier family members enrolled in DIAN as controls for image analysis. We included the additional ADRC cohort patients because the DIAN dataset contained relatively few cases who had established dementia at study entry.

DIAN is a multicenter study of individuals from families with known causative mutations for DIAD. Enrolled family members undergo initial genotyping and clinical reassessment every one or more years, including neuroimaging. Subjects can be DIAD-MC or non-carrier family members. The DIAN study receives approval from the institutional review board (IRB) of each participating site. Written informed consent is obtained from all participants or their designated guardians.[8]

TABLE 1 Participant demographics and genotype (of three mutated genes causing dominantly inherited Alzheimer's disease)

	Control group	Training group			Testing group		
	CDR 0	CDR 0	CDR≥ 1		CDR 0	CDR 0.5	Converters[a]
Cohort	DIAN	DIAN	DIAN	ADRC[b]	DIAN	DIAN	DIAN
N (visits)	99 (99)	123 (123)	28 (28)	15 (15)	15 (54)	20 (57)	30 (95)
Follow up Mean ± SD (years)	2.9 ± 3.4	2.79 ± 1.09	1.56 ± 1.36	NA	5.01 ± 1.23	3.15 ± 1.52	2.39 ± 1.35
PSEN1	NA	87	22	15	11	13	21
PSEN2	NA	15	0	0	0	0	3
APP	NA	21	6	0	4	7	6
Age Mean ± SD (years)	38 ± 11.3	33.6 ± 9.5	48.7 ± 8.8	43 ± 6.1	39.2 ± 9.8	47.2 ± 10.7	43.2 ± 9.0
Male %	41 (41%)	56 (45.5%)	14 (50%)	9 (60.0%)	4 (26.6%)	5 (25%)	11 (36.6%)

Abbreviations: ADRC, Alzheimer's Disease Research Center; *APP*, amyloid precursor protein; CDR, Clinical Dementia Rating; DIAN, Dominantly Inherited Alzheimer Network; *PSEN*, presenilin; SD, standard deviation; UCLA, University of California Los Angeles; USC, University of Southern California.
[a]Refers to subjects from the ADRC-UCLA and ARDC-USC.
[b]Converters refers to subject who converted from CDR 0 or from CDR 0.5 to CDR 1, 2, or 3, and to subjects who converted from CDR 0 to CDR 0.5.

The ADRC-UCLA and ADRC-USC are both National Institute on Aging–designated research centers that offer extensive clinical, neuroimaging, and molecular profiling of patients with dementia, including DIAD-MC.[24] In the case of DIAD-MC evaluated in ADRC-UCLA or ADRC-USC, the study was approved by each institution's IRB. Subjects or their proxies gave written approval for study participation.[13]

Our inclusion criteria included availability of the following data for each individual: age, sex, and functional status data as expressed in Clinical Dementia Rating Global Score (henceforth referred to as CDR), and one or more 3-Tesla T1 structural MRIs.

The 231 DIAD-MC were divided into two groups. A training group (n = 166) was created to identify the atrophy pattern associated with dementia and develop a dementia risk score. This group consisted of 123 participants with CDR = 0 and 43 patients with CDR ≥1 at their first visit. To maximize the likelihood that the images from the CDR = 0 group represented the asymptomatic phase of disease, we only included individuals with a CDR = 0 rating for two consecutive visits. The first study image from each participant was used for training. The testing group consisted of 65 DIAD-MC who did not have dementia at study entry and who were followed longitudinally, and whose images were used to test the risk score. Table 1 summarizes the groups and the amount of DIAD-MC in each.

2.3 | Clinical and genetic assessment

Functional status was determined using the CDR. Each individual's CDR represents a weighted average of six functional domains (memory, orientation, judgment and problem solving, community affairs, home and hobbies, personal care). The scale categorizes individuals as asymptomatic (CDR = 0), having very mild symptoms that do not impair independent functioning (CDR = 0.5), or clear symptoms of dementia (CDR ≥ 1). Genotyping methods have been previously described.[8,13]

The mutation-EYO is a variable that estimates the time until symptom onset and is calculated at each visit by subtracting the participant's age from the mean age of symptom onset for their specific mutation[7] (i.e., negative values indicate conversion is expected to occur in the future).

2.4 | Image acquisition

Participants in the DIAN study underwent 3-Tesla volumetric T1-weighted MRI according to the Alzheimer's Disease Neuroimaging Initiative (ADNI)–defined sequences.[25] Matching between scanners and image quality control were performed according to the ADNI protocol by the study imaging core.[8] Participants of the ADRC-UCLA and ADRC-USC underwent similar MRI acquisition protocols (see Table S1 in supporting information).

2.5 | Image processing

For this study we only analyzed T1-weighted images. We excluded all images with excessive motion and imaging artifacts, as determined by visual inspection. We corrected for magnetic field bias using the N3 algorithm.[26] We segmented the remaining images using the unified segmentation procedure in Statistical Parametric Mapping (SPM) version 12 into gray matter (GM), white matter, and CSF.[27]

The next steps in image processing depended on whether the participant contributed an image from a single observation or multiple longitudinal observations. For the training group, a study-specific template representative of all participants was generated from T1 GM images using diffeomorphic anatomical registration using exponentiated lie algebra.[28]The images were subsequently normalized and modulated in the study-specific template space using linear and non-linear registration.

For the testing group, an additional step included creation of an intraparticipant template using nonlinear diffeomorphic and rigid body registration implemented with SPM.[29] This process minimizes bias in

estimating change in volume over time.[27] The group template for this group was generated from the within-participant averaged GM, white matter, and CSF tissue maps by nonlinear and rigid-body registration.

All images were then warped into a group template space and smoothed with a 4 mm isotropic Gaussian kernel. We calculated total intracranial volume (TIV) for each participant in group template space.

2.6 | Calculation of atrophy burden

For every processed image, we estimated atrophy in each GM voxel by regional voxel estimates of volume relative to a control group of 99 non-carrier asymptomatic family members from the DIAN study. This was done to create a *W*-score, which is similar to a *z*-score and represents a standardized estimate of atrophy at that voxel after accounting for age and TIV.[30] We summed the voxel-wise *W*-scores within 179 regions of interest (ROI), as defined by the Desikan brain atlas[31] to create a measure of atrophy burden for each ROI.

2.7 | Generation of DIAD atrophy-based dementia risk score

The concept and method for generating an atrophy-based dementia risk score (henceforth risk score) from *w*-scores has been described in detail previously.[23] Briefly, we created *w*-score based regional measures of atrophy burden, as described above, from the earliest images obtained from individuals in the training group. The regional atrophy burden estimates from the asymptomatic and CDR $\geq$ 1 cases in the training group were entered into an L2-regularized logistic regression algorithm,[32] with diagnosis as the categorical outcome. The algorithm was implemented in a machine learning Python package using the fast incremental gradient method.[33,34]The probability distribution formula and method of optimizing the empirical log-logistic have been previously described.[23] To estimate model performance a five-fold cross-validation scheme was used,[35] as previously described.[23] The predicted outcome from the fitted logistic regression equation is a risk score that ranges from 0 to 1 and represents the probability of either being demented or asymptomatic. To test the accuracy of our risk in separating asymptomatic from DIAD-MC with dementia we dichotomized individual scores above 0.5 as approximating dementia and below 0.5 approximating asymptomatic individuals. We compared risk score–based approximation of symptoms to actual symptoms in each individual. The risk score accuracy was calculated as the proportion of patients correctly classified.

2.8 | Testing the utility of the risk score

We next assessed the utility of the risk score and mutation-EYO for predicting dementia onset in the testing group using two methods: a Cox regression model and a receiver operating characteristic (ROC) curve. Risk scores were calculated from all images in the testing group, which included carriers who started at a CDR 0 or 0.5 and were followed longitudinally.

We used a Cox regression model with atrophy risk score and mutation-EYO as time-varying predictors and conversion from CDR = 0 or CDR = 0.5 to CDR $\geq$ 1 as the outcome. Sex was added as a covariate in these models. To quantify the relationship between risk score and outcome, we estimated the effect of a 10% increase in the risk score (increase in value of 0.1). A Kaplan–Meier curve was constructed for this model with individual scores dichotomized above and below risk score value 0.5; this value was chosen for illustrative purposes. We also tested an interaction effect of risk score by mutation-EYO in a second model.

In addition, we evaluated and compared the risk scores and mutation-EYO performance in identifying DIAD-MC who converted from either CDR 0 or 0.5 to CDR $\geq$ 1 within 25 months of their baseline visit using a ROC curve. This time frame was chosen to approximate duration of some disease-modifying drug trials that might target prevention of dementia. For this analysis, we included the same individuals as in the Cox regression model. We dichotomized the risk scores above 0.5 and the mutation-EYO value higher than negative 25 months as predicting change from CDR = 0 or 0.5 to CDR $\geq$ 1. This technique fits a maximum likelihood ROC model using a binormal distribution of the true state of the observation (progressed vs. not progressed). The ROC models were fitted using Stata v16.1.

3 | RESULTS

3.1 | Participants

The study group included 231 DIAD-MC and 99 non-carrier family members. Of these, 166 DIAD-MC were included in the training group for generating the logistic model risk score (124 *PSEN1*, 15 *PSEN2*, and 27 *APP*) and 65 in the testing group for survival analysis (45 *PSEN1*, 3 *PSEN2*, and 17 *APP*). Table 1 summarizes the age and sex by symptom severity for each analysis used, including the control group.

3.2 | Atrophy-based dementia risk score generation

The training group consisted of 43 DIAD-MC with CDR $\geq$ 1 and 123 with CDR = 0 for two consecutive visits, and a mean time on CDR = 0 of 2.79 $\pm$ 1.09 years. Figure 1 shows the optimal weight each brain region is given as a covariate in the logistic regression formula for the risk score. An ROI's weight indicates its reliability in separating CDR = 0 and CDR $\geq$ 1. Table 2 lists the 50 ROIs with highest absolute weight alongside their mean standardized atrophy in DIAD-MC with CDR $\geq$ 1. As expected, subregions of the medial temporal, precuneus, temporoparietal, and dorsolateral frontal regions comprised most of the list and showed the largest degree of atrophy, but high weights for prediction were also observed in subcortical regions such as the cerebellar cortices, globus pallidi, and caudate nuclei. Our model achieved good

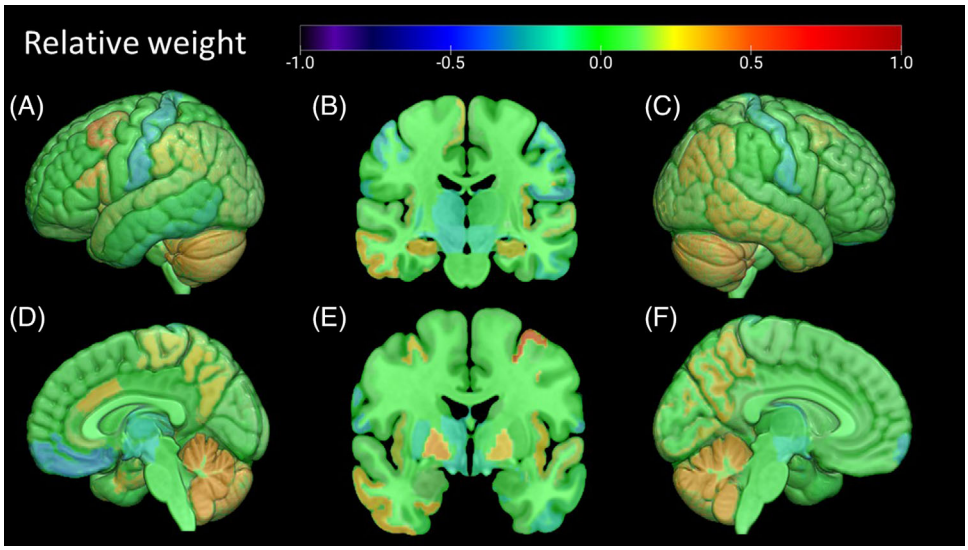

FIGURE 1 Brain map displaying the relative weight (color coded) each region of interest (ROI) is given in the atrophy-based dementia risk score. Individual ROI weights were the result of the optimization of the logistic regression model. These weights were subsequently used to calculate prediction scores for the survival analysis. The weight indicates the degree of reliability of an ROI in separating presymptomatic and demented dominantly inherited Alzheimer's disease mutation carriers. An ROI with a high positive or negative weight increases the probability that a given individual with atrophy in this region is Clinical Dementia Rating (CDR) scale ≥ 1 or CDR = 0 respectively, whereas a weight closer to zero or zero indicates the ROI is less relevant for separating between these two outcomes. A and D, Left lateral and medial views, respectively. C and F, Right lateral and medial views, respectively. B and E, Hippocampal and basal ganglia level coronal slices, respectively

separation of symptomatic DIAD-MC based on risk score cutoff above 0.5 with a 96.4% (standard error [SE] = 0.02).

3.3 | Predicting symptom onset

The hazard ratio (HR) for our Cox model was 1.31 (95% confidence interval [CI] 1.14–1.49, $P < .001$), indicating higher risk and shorter time to conversion with increasing risk score. Results of Kaplan–Meier curve for the Cox model, after dichotomizing the risk score using a threshold of 0.5, can be seen in Figure 2. The HR for mutation-EYO was 1.18 (95% CI 1.03–1.35, $P = .017$). Sex was not a statistically significant predictor of survival (HR = 0.41, 95% CI 0.15–1.16, $P = .093$), but was in the direction of greater risk for males. There was no significant interaction between mutation-EYO and risk score ($P = .88$). The ROC area under the curve (AUC) was 0.903 (0.823–0.982) for the risk score, 0.825 (0.724–0.927) for the EYO, and 0.910 (0.830–0.990) for both (Figure 3).

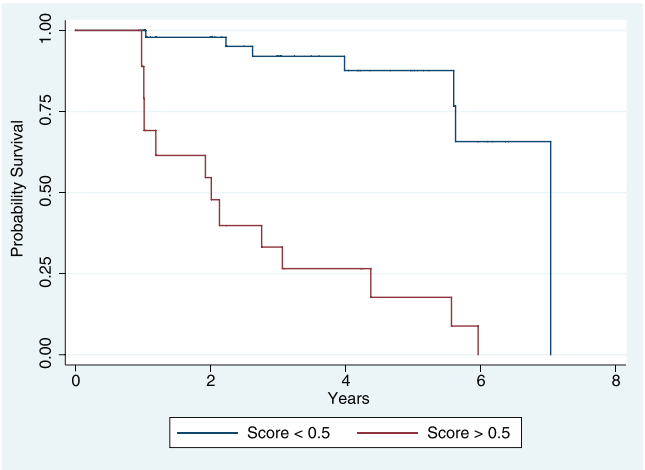

FIGURE 2 Kaplan–Meier curve of displaying dominantly inherited Alzheimer's disease mutation carriers survival from Clinical Dementia Rating (CDR) scale 0 or 0.5 to CDR 1. Mutation carriers were dichotomized using the atrophy-based dementia risk score values above and below 0.5 (red and blue, respectively)

4 | DISCUSSION

Our aim was to determine whether individualized atrophy-based risk scores from a single observation could predict onset of dementia in DIAD-MC. Our developed risk score separated asymptomatic DIAD-MC from those with dementia with an accuracy of 96.4%. Moreover, in an independent subset of asymptomatic and mildly symptomatic DIAD-MC with longitudinal observations, every 0.1 unit increase in our risk score (a 10% increase) translated to roughly 1.3-fold increased likelihood of converting to dementia. Last, the risk score was useful in identifying asymptomatic DIAD-MC that converted to dementia within 2 years with 90.3% accuracy, and achieved 91% accuracy when combined with the EYO.

These findings are consistent with and extend prior work. In particular, previous studies have shown that hippocampal volumes and decline in hippocampal and whole brain cortical volumes, as well as other biomarkers, predict decline in DIAD-MC.[6,8,10–13,36] To our knowledge

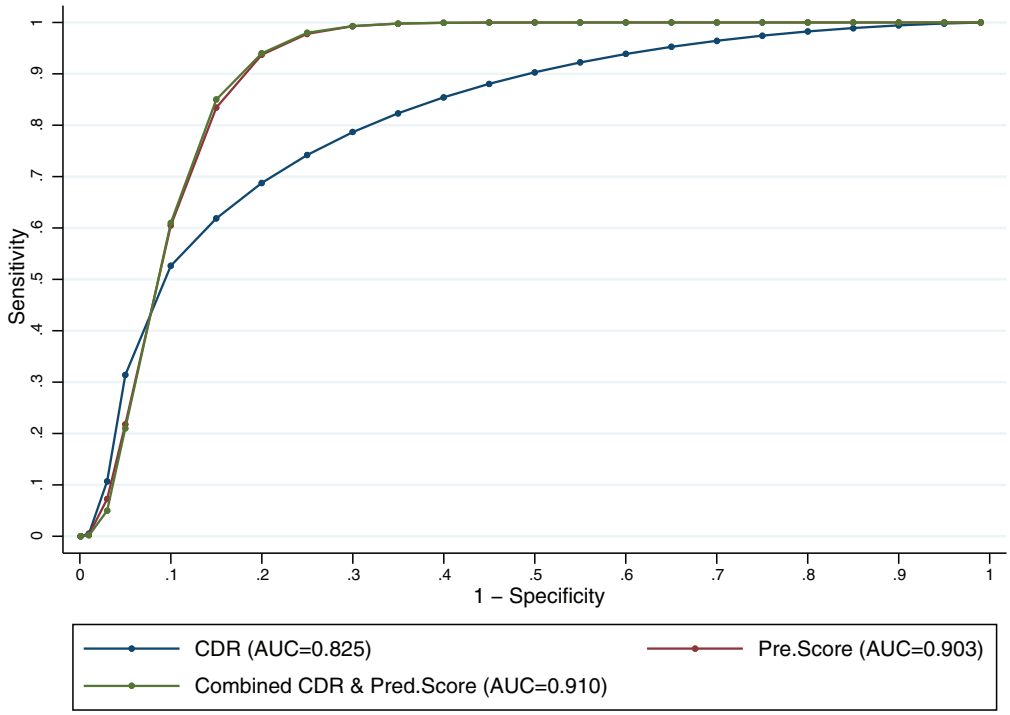

FIGURE 3 Receiver operating curve for conversion to dementia within 25 months in dominantly inherited Alzheimer's disease mutation carriers based on: the Dominantly Inherited Alzheimer Network estimated years to onset variable (blue), brain atrophy–based dementia risk score (green), and both (red). AUC, area under the curve; CDR, Clinical Dementia Rating

this is the first study demonstrating the utility of single measurements of cerebral GM for predicting dementia onset, a critical event in the evolution of disease, in DIAD-MC.

Our results suggest that individualized atrophy-based dementia risk scores could help address several challenges in developing treatments for AD. The age of symptom onset can vary by many years in DIAD-MC even within carriers of the same type of DIAD mutation.[7] Trials seeking to delay dementia onset must identify individuals that will develop symptoms within a short, defined time frame. An atrophy-based risk score may be useful for selecting mutation carriers that are closest to dementia conversion. This can help avoid unnecessary inclusion of individuals at low risk for dementia within 2 to 3 years in studies of DIAD-MC and increase trial power. Moreover, individual atrophy maps and risk scores can theoretically be used to follow recruited subjects for progression throughout trials. Proximity to dementia onset may also be used to inform clinical care of DIAD-MC.

Our approach is similar to prior analyses that used baseline atrophy patterns to predict dementia in sporadic AD.[22,37] Many of these studies were conducted using data from the ADNI.[22,38,39] This database comprises individuals with sporadic AD that are on average 30 to 40 years older than most DIAD-MC. Brain atrophy in DIAD-MC can occur in areas not typically associated with sporadic AD, such as the putamen and thalamus.[10] Thus, models relying on atrophy in sporadic AD, particularly in predetermined ROI,[21,38,40] might not be generalizable to DIAD populations. This justified an empirical approach to identify the most valuable regions for predicting dementia in DIAD. Our method is designed to identify regions that predict onset of dementia without reliance on a priori ROI. Indeed, although our analysis showed that the temporal, parietal, and frontal regions showed the highest degree of atrophy and predicted onset of dementia, as would be expected based on sporadic AD (Figure 1, Table 2), regions not typically atrophic in sporadic AD, such as the cerebellar cortices, globus pallidi, and caudate nuclei also contributed to prediction. The highest contribution of atypical ROI was from the cerebellar cortices, although it should be noted that the combined contributions of atypical subcortical regions was smaller than for the typical AD regions taken together. While cerebellar GM volume in DIAD-MC with dementia was reliably lower than that of asymptomatic DIAD-MC, regions typical of sporadic AD were on average more atrophic and together contributed more to the risk score (Table 2). Cerebellar atrophy is generally understudied in AD and DIAD. It has been previously described in some studies of DIAD-MC,[10,16,41] but many studies have relied on surface-based methods that exclude the cerebellum from analysis.[14,15]

Our current methods have several limitations that could be addressed in future analyses to improve utility. Accuracy of the risk score can be increased by using a larger sample size. To generate our risk score we pooled three different DIAD genes (with 67 different mutations) to maximize our sample size. Building this model in each gene separately would likely increase risk score accuracy but would require a larger sample size. Furthermore, the relative value of imaging-based predictors compared to mutation-EYO may vary by mutation. The risk score was generated from neuroimaging data of 43 DIAD-MC with dementia; of these 12 had a CDR of 2 or 3. Using neuroimaging data from DIAD carriers at earliest conversion to CDR of

TABLE 2 The 50 ROI of highest absolute weight given in the atrophy-based dementia risk score alongside the ROI's mean standardized atrophy (W-score) in DIAD-MC with CDR >1

Gray matter regions of interest (Desikan-Killiany Atlas)	Weight	*W*-scores in CDR ≥ 1 (mean ± SD)
Caudal middle frontal left	0.5747	−0.79 ± 0.58
Cerebellum left	0.5111	−0.61 ± 1.14
Inferior temporal right	0.4847	−1.07 ± 0.64
Banks superior temporal sulcus left	0.4803	−1.39 ± 0.8
Caudal middle frontal right	0.44	−0.69 ± 0.64
Entorhinal right	0.3732	−1.22 ± 1.14
Pallidum right	0.3643	−0.17 ± 0.12
Inferior parietal right	0.3557	−1.26 ± 0.72
Precuneus right	0.3466	−1.6 ± 0.68
Middle temporal right	0.3432	−1.29 ± 0.79
Cerebellum right	0.3356	−0.6 ± 1.02
Caudal anterior cingulate right	0.3228	−0.74 ± 0.81
Precuneus left	0.3012	−1.57 ± 0.66
Pars oercularis left	0.298	−0.67 ± 0.66
Insula left	0.2961	−0.84 ± 0.79
Pallidum left	0.2933	−0.29 ± 0.19
Hippocampus right	0.2859	−1.8 ± 1.22
Inferior parietal left	0.2593	−1.18 ± 0.71
Superior parietal right	0.2573	−1.02 ± 0.51
Rostral middle frontal right	0.2422	−0.74 ± 0.65
Paracentral right	0.2267	−1.09 ± 0.81
Pars opercularis right	0.2245	−0.58 ± 0.71
Supramarginal left	0.2237	−1.3 ± 0.82
Lateral orbital frontal left	0.2145	−0.6 ± 0.77
Lateral occipital left	0.2127	−1.29 ± 0.62
Lingual left	0.2106	−1.27 ± 0.77
Insula right	0.2096	−0.94 ± 0.91
Superior temporal left	0.2081	−1.17 ± 0.78
Cuneus left	0.2072	−1.44 ± 0.78
Caudate left	0.2061	−0.73 ± 0.94
Cuneus right	0.1955	−1.68 ± 0.71
Superior temporal right	0.1879	−1.21 ± 0.88
Lingual right	0.1814	−1.34 ± 0.72
Hippocampus left	0.1767	−1.81 ± 1.17
Superior frontal right	0.1754	−0.55 ± 0.67
Lateral occipital right	0.155	−1.2 ± 0.7
Amygdala right	0.1542	−2.04 ± 1.69
Isthmus cingulate left	0.1541	−1.64 ± 0.83
Rostral anterior cingulate right	0.1454	−0.78 ± 0.82
Posterior-cingulate left	0.1433	−1.53 ± 0.72
Parahippocampal right	0.1428	−0.88 ± 1.04
Rostral anterior cingulate left	0.1414	−0.77 ± 0.76
Inferior temporal	-0.143	−1.04 ± 0.71
Putamen right	-0.1533	−1.56 ± 1.12
Frontal pole left	-0.1601	−0.64 ± 0.81
Ventral diencephalon right	-0.1868	−0.49 ± 0.4
Thalamus right	-0.2259	−1.23 ± 0.83
Postcentral left	-0.2306	−1.06 ± 0.71
Postcentral right	-0.251	−1.28 ± 0.78
Medial orbital frontal right	-0.2833	−0.73 ± 0.82

Abbreviations: CDR, Clinical Dementia Rating; DIAD-MC, dominantly inherited Alzheimer's disease mutation carrier; ROI, region of interest; SD, standard deviation.

Notes: Individual ROI weights were the result of the optimization of the logistic regression model. The weight indicates the degree of reliability of an ROI in separating presymptomatic and demented DIAD mutation carriers and does not necessarily correlate with the degree of atrophy.

An ROI with a high positive or negative weight increases the probability that a given individual with atrophy in this region is CDR ≥ 1 or CDR = 0, respectively, whereas a weight closer to zero or zero indicates the ROI is less relevant for separating these two outcomes.

one might improve the sensitivity of this risk score. Another limitation is the use of dementia as a binary outcome, and future trials may use time to reach an earlier, cognitively defined threshold. Nevertheless, cognitive impairment as defined by CDR is still the major outcome in most AD clinical trials. Last, while T1-weighted MRI and EYO already provide a high degree of accuracy, other neuroimaging measures,[6,8,41,42,10–16,19] biochemical,[6,8,12,18,43] or other markers of AD[44] can potentially be added to the model to improve accuracy.

With all of these enhancements, prediction scores can be developed into a powerful tool for clinical trials and may also facilitate treatment planning in DIAD-MC and other people with high risk for developing dementia.

ACKNOWLEDGMENTS

This research was supported by the National Institutes of Health, grants P01 AG019724, - P30 AG062422, K24 AG045333, U19 AG063911, U01 AG045390, U54 NS092089, U01AG051218, P50AG016570, P50AG005142, K08AG022228, P30 AG066444; P01 AG03991; P01 AG026276; U19 AG032438, P30 AG010133, R01 AG019771, P30 AG010133, R01 AG019771, R01 AG057739, U01 AG024904, R01 LM013463, R01 AG068193, and U01 AG068057 and the Alzheimer's Association research fellowship to promote diversity grant AARFD-20-681815. Data collection and sharing for this project was supported by The Dominantly Inherited Alzheimer Network (DIAN, UF1AG032438) funded by the National Institute on Aging (NIA), the German Center for Neurodegenerative Diseases (DZNE), Raul Carrea Institute for Neurological Research (FLENI), with partial support by the Research and Development Grants for Dementia from

Japan Agency for Medical Research and Development, AMED, and the Korea Health Technology R&D Project through the Korea Health Industry Development Institute (KHIDI). This manuscript has been reviewed by DIAN Study investigators for scientific content and consistency of data interpretation with previous DIAN Study publications. We acknowledge the altruism of the participants and their families and contributions of the DIAN research and support staff at each of the participating sites for their contributions to this study.

CONFLICTS OF INTEREST

Dr. Clifford Jack serves on an independent data monitoring board for Roche and has consulted for Eisai, but he receives no personal compensation from any commercial entity. He receives research support from NIH and the Alexander Family Alzheimer's Disease Research Professorship of the Mayo Clinic. Dr. Saykin receives support from Arkley BioTek (joint NIH SBIR grant); Avid Radiopharmaceuticals (in kind contribution of PET tracer precursor); Bayer Oncology (Scientific Advisory Board); Eli Lilly (collaborative research grant); and Springer-Nature Publishing (Editorial Office Support as Editor in Chief, *Brain Imaging and Behavior*). Ophir Keret is an Atlantic Fellow for Equity in Brain Health and thanks the Global Brain Health Institute for supporting his work. Johannes Levin reports speaker fees from Bayer Vital and Roche; consulting fees from Axon Neuroscience; author fees from Thieme medical publishers and W. Kohlhammer GmbH medical publishers; non-financial support from Abbvie; and compensation for duty as part-time CMO from MODAG, outside the submitted work. John C. Morris reports support from NIH grants P30 AG066444, P01 AG003991, and P01 AG026276 during the conduct of the study. He serves on the Editorial Boards of *Brain & Life* and *Alzheimer's & Dementia*. Su Yi was a paid consultant for Green Valley Pharmaceuticals LLC in 2018. Adam M. Staffaroni provides consultation to Takeda and receives research funding from the NIH, the Larry L. Hillblom Foundation, and the Bluefield Project to Cure FTD. Stephan Salloway reports grants, personal fees, and non-financial support from Biogen; grants and personal fees from Eisai; grants, personal fees, and non-financial support from Avid; personal fees and non-financial support from Novartis; grants, personal fees, and non-financial support from Lilly; personal fees from Genentech; personal fees and non-financial support from Roche, outside the submitted work. Michael Weiner receives support for his work from the following funding sources: NIH, DOD, PCORI, California Dept. of Public Health, U. Michigan, Siemens, Biogen, Hillblom Foundation, Alzheimer's Association, The State of California, Johnson & Johnson, Kevin and Connie Shanahan, GE, VUmc, Australian Catholic University (HBI-BHR), The Stroke Foundation, Fidelity Charitable, and the Veterans Administration. Dr. Weiner has served on advisory boards for Cerecin/Accera, Alzheon, Inc., Nestle/Nestec, PCORI/PPRN, Dolby Family Ventures, National Institute on Aging (NIA), Boston University Alzheimer's Disease and CTE Center, MIRIADE at VUmc for Amsterdam UMC, Cytox, Indiana University, Acumen, Brain Health Registry and ADNI. He serves on the Editorial Boards for Alzheimer's & Dementia, TMRI and MRI. He has provided consulting and/or acted as a speaker/lecturer to Cerecin/Accera, Inc., Alzheimer's Drug Discovery Foundation (ADDF), BioClinica, The Buck Institute for Research on Aging, FUJIFILM-Toyama Chemical (Japan), Garfield Weston, Baird Equity Capital, University of Southern California (USC), T3D Therapeutics, Cytox, Guidepoint, and Japanese Organization for Medical Device Development, Inc. (JOMDD). He holds stock options with Alzheon, Inc., Alzeca, and Anven. Bruce L. Miller reported serving on the advisory committee for Cambridge National Institute for Health Research Biomedical Research Centre; serving on the board of directors for J Douglas French Alzheimer's Foundation and Safely You; serving as medical advisor and receiving grant support from The Bluefield Project for Frontotemporal Dementia Research; consulting for Rainwater Charitable Foundation, Stanford Alzheimer's Disease Research Center, Buck Institute, Larry L. Hillblom Foundation, University of Texas Center for Brain Health, University of Washington Alzheimer's Disease Research Center, and Harvard University Alzheimer's Disease Research Center; receiving royalties from Guilford Press, Cambridge University Press, Johns Hopkins Press, and Oxford University Press; serving as editor for *Neurocase*; serving as section editor for *Frontiers in Neurology*; and receiving grants P30 AG062422, P01 AG019724, R01 AG057234, and T32 AG023481 from the NIH. Gil D. Rabinovici receives research support from Avid Radiopharmaceuticals, Eli Lilly, GE Healthcare, Genentech, Life Molecular Imaging. He has received consulting fees from Axon Neurosciences, Eisai, Genentech, GE Healthcare, Miller Medical Communications, Roche. He is an Associate Editor for *JAMA Neurology*. Howard J. Rosen reported consulting for Wave Neuroscience outside the submitted work. All other authors have no potential conflicts to disclose.

REFERENCES

1. Honig LS, Vellas B, Woodward M, et al. Trial of solanezumab for mild dementia due to Alzheimer's disease. *N Engl J Med*. 2018;378(4):321-330.
2. Egan MF, Kost J, Tariot PN, et al. Randomized trial of verubecestat for mild-to-moderate Alzheimer's disease. *N Engl J Med*. 2018;378(18):1691-1703.
3. Sperling RA, Jack CR, Aisen PS. Testing the right target and right drug at the right stage. *Sci Transl Med*. 2011;3(111):111cm33. https://doi.org/10.1126/scitranslmed.3002609.
4. Sperling RA, Rentz DM, Johnson KA, et al. The A4 study: stopping AD before symptoms begin?. *Sci Transl Med*. 2014;6(228):228fs13. https://doi.org/10.1126/scitranslmed.3007941.
5. Weninger S, Carrillo MC, Dunn B, et al. Collaboration for Alzheimer's Prevention: principles to guide data and sample sharing in preclinical Alzheimer's disease trials. *Alzheimer's Dement*. 2016;12(5):631-632. https://doi.org/10.1016/j.jalz.2016.04.001.
6. McDade E, Wang G, Gordon BA, et al. Longitudinal cognitive and biomarker changes in dominantly inherited Alzheimer disease. *Neurology*. 2018;91(14):e1295-e1306. https://doi.org/10.1212/WNL.0000000000006277.
7. Ryman DC, Acosta-Baena N, Aisen PS, et al. Symptom onset in autosomal dominant Alzheimer disease: a systematic review and meta-analysis. *Neurology*. 2014;83(3):253-60. https://doi.org/10.1212/WNL.0000000000000596.
8. Bateman RJ, Xiong C, Benzinger TLS, et al. Clinical and biomarker changes in dominantly inherited Alzheimer's disease. *N Engl J Med*. 2012;367:795-804. https://doi.org/10.1056/NEJMoa1202753.
9. Jack CR, Knopman DS, Jagust WJ, et al. Hypothetical model of dynamic biomarkers of the Alzheimer's pathological cascade. *Lancet*

Neurol. 2010;9(1):119-128. https://doi.org/10.1016/S1474-4422(09)70299-6.
10. Cash DM, Ridgway GR, Liang Y, et al. The pattern of atrophy in familial alzheimer disease: volumetric MRI results from the DIAN study. *Neurology*. 2013;81(16):1425-33. https://doi.org/10.1212/WNL.0b013e3182a841c6.
11. Kinnunen KM, Cash DM, Poole T, et al. Presymptomatic atrophy in autosomal dominant Alzheimer's disease: a serial magnetic resonance imaging study. *Alzheimer's Dement*. 2018;14(1):43-53. https://doi.org/10.1016/j.jalz.2017.06.2268.
12. Wang G, Xiong C, McDade EM, et al. Simultaneously evaluating the effect of baseline levels and longitudinal changes in disease biomarkers on cognition in dominantly inherited Alzheimer's disease. *Alzheimer's Dement Transl Res Clin Interv*. 2018;4(1):669-676. https://doi.org/10.1016/j.trci.2018.10.009.
13. Lee GJ, Lu PH, Medina LD, et al. Regional brain volume differences in symptomatic and presymptomatic carriers of familial Alzheimer's disease mutations. *J Neurol Neurosurg Psychiatry*. 2013;84(2):154–162. https://doi.org/10.1136/jnnp-2011-302087.
14. Gordon BA, Blazey TM, Su Y, et al. Spatial patterns of neuroimaging biomarker change in individuals from families with autosomal dominant Alzheimer's disease: a longitudinal study. *Lancet Neurol*. 2018;17(3):241-250. https://doi.org/10.1016/S1474-4422(18)30028-0.
15. Benzinger TLS, Blazey T, Jack CR, et al. Regional variability of imaging biomarkers in autosomal dominant Alzheimer's disease. *Proc Natl Acad Sci U S A*. 2013;110(47):E4502-E4509. https://doi.org/10.1073/pnas.1317918110.
16. Fortea J, Sala-Llonch R, Bartrés-Faz D, et al. Increased cortical thickness and caudate volume precede atrophy in psen1 mutation carriers. *J Alzheimer's Dis*. 2010;22(3):909-922. https://doi.org/10.3233/JAD-2010-100678.
17. Quiroz YT, Stern CE, Reiman EM, et al. Cortical atrophy in presymptomatic Alzheimer's disease presenilin 1 mutation carriers. *J Neurol Neurosurg Psychiatry*. 2013;84(5):556–561. https://doi.org/10.1136/jnnp-2012-303299.
18. Llibre-Guerra JJ, Li Y, Schindler SE, et al. Association of longitudinal changes in cerebrospinal fluid total tau and phosphorylated tau 181 and brain atrophy with disease progression in patients with Alzheimer disease. *JAMA Netw Open*. 2019;2(12):e1917126. https://doi.org/10.1001/jamanetworkopen.2019.17126.
19. Gordon BA, Blazey TM, Christensen J, et al. Tau PET in autosomal dominant Alzheimer's disease: relationship with cognition, dementia and other biomarkers. *Brain*. 2019;142(4):1063–1076. https://doi.org/10.1093/brain/awz019.
20. Braak H, Braak E. Neuropathological stageing of Alzheimer-related changes. *Acta Neuropathol*. 1991;82:239–259. https://doi.org/10.1007/BF00308809.
21. McEvoy LK, Fennema-Notestine C, Roddey JC, et al. Alzheimer disease: quantitative structural neuroimaging for detection and prediction of clinical and structural changes in mild cognitive impairment. *Radiology*. 2009;251(1):195-205. https://doi.org/10.1148/radiol.2511080924.
22. Dickerson BC, Wolk DA. Biomarker-based prediction of progression in MCI: comparison of AD signature and hippocampal volume with spinal fluid amyloid-beta and tau. *Front Aging Neurosci*. 2013;5(1): 55.
23. Staffaroni AM, Cobigo Y, Goh SYM, et al. Individualized atrophy scores predict dementia onset in familial frontotemporal lobar degeneration. *Alzheimer's Dement*. 2020;16(1):37-48. https://doi.org/10.1016/j.jalz.2019.04.007.
24. National Institute on Aging - Alzheimer's Disease Research Centers n.d.
25. Jack CR, Bernstein MA, Fox NC, et al. The Alzheimer's disease neuroimaging initiative (ADNI): mRI methods. *J Magn Reson Imaging*. 2008;27(4):685-691. https://doi.org/10.1002/jmri.21049.
26. Zheng W, Chee MWL, Zagorodnov V. Improvement of brain segmentation accuracy by optimizing non-uniformity correction using N3. *Neuroimage*. 2009;48(1):73-83. https://doi.org/10.1016/j.neuroimage.2009.06.039.
27. Kurth F, Gaser C, Luders E. A 12-step user guide for analyzing voxel-wise gray matter asymmetries in statistical parametric mapping (SPM). *Nat Protoc*. 2015;10:293–304. https://doi.org/10.1038/nprot.2015.014.
28. Ashburner J. A fast diffeomorphic image registration algorithm. *Neuroimage*. 2007;38(1):95-113. https://doi.org/10.1016/j.neuroimage.2007.07.007.
29. Ashburner J, Ridgway GR. Symmetric diffeomorphic modeling of longitudinal structural MRI. *Front Neurosci*. 2013;6:197. https://doi.org/10.3389/fnins.2012.00197LK.
30. Jack CR, Petersen RC, Xu YC, et al. Medial temporal atrophy on MRI in normal aging and very mild Alzheimer's disease. *Neurology*. 1997;49(3):786-94. https://doi.org/10.1212/WNL.49.3.786.
31. Desikan RS, Ségonne F, Fischl B, et al. An automated labeling system for subdividing the human cerebral cortex on MRI scans into gyral based regions of interest. *Neuroimage*. 2006;31(3):968-980.
32. Liu J, Chen J, Ye J. Large-scale sparse logistic regression. Proc. ACM SIGKDD Int. Conf. Knowl. Discov. Data Min. 2009. https://doi.org/10.1145/1557019.1557082
33. Pedregosa F, Varoquaux G, Gramfort A, et al. Scikit-learn: machine learning in Python. *J Mach Learn Res*. 2011;12.
34. Defazio A, Bach F, Lacoste-Julien S. SAGA: a fast incremental gradient method with support for non-strongly convex composite objectives. *Adv Neural Inf Process Syst*. 2014.
35. Fushiki T. Estimation of prediction error by using K-fold cross-validation. *Stat Comput*. 2011;21:137–146. https://doi.org/10.1007/s11222-009-9153-8.
36. Lee YEC, Williams DR, Anderson JFI. Frontal deficits differentiate progressive supranuclear palsy from Parkinson's disease. *J Neuropsychol*. 2016;10(1):1-14. https://doi.org/10.1111/jnp.12053.
37. Desikan RS, Cabral HJ, Settecase F, et al. Automated MRI measures predict progression to Alzheimer's disease. *Neurobiol Aging*. 2010;31(8):1364-1374. https://doi.org/10.1016/j.neurobiolaging.2010.04.023.
38. Jack CR, Wiste HJ, Vemuri P, et al. Brain beta-amyloid measures and magnetic resonance imaging atrophy both predict time-to-progression from mild cognitive impairment to Alzheimer's disease. *Brain*. 2010;133(11):3336–3348,. https://doi.org/10.1093/brain/awq277.
39. Hinrichs C, Singh V, Xu G, Johnson SC. Predictive markers for AD in a multi-modality framework: an analysis of MCI progression in the ADNI population. *Neuroimage*. 2011;55(2):574-589. https://doi.org/10.1016/j.neuroimage.2010.10.081.
40. McEvoy LK, Holland D, Hagler DJ, Fennema-Notestine C, Brewer JB, Dale AM. Mild cognitive impairment: baseline and longitudinal structural MR imaging measures improve predictive prognosis. *Radiology*. 2011;259(3). https://doi.org/10.1148/radiol.11101975.
41. Reiman EM, Quiroz YT, Fleisher AS, et al. Brain imaging and fluid biomarker analysis in young adults at genetic risk for autosomal dominant Alzheimer's disease in the presenilin 1 E280A kindred: a case-control study. *Lancet Neurol*. 2012;11(12):1048-1056. https://doi.org/10.1016/S1474-4422(12)70228-4.
42. Montal V, Vilaplana E, Alcolea D, et al. Cortical microstructural changes along the Alzheimer's disease continuum. *Alzheimer's Dement*. 2018;14(3):340-351. https://doi.org/10.1016/j.jalz.2017.09.013.
43. Quiroz YT, Zetterberg H, Reiman EM, et al. Plasma neurofilament light chain in the presenilin 1 E280A autosomal dominant Alzheimer's disease kindred: a cross-sectional and longitudinal cohort study. *Lancet Neurol*. 2020;19(6):513-521. https://doi.org/10.1016/S1474-4422(20)30137-X.

44. Guzmán-Vélez E, Jaimes S, Aguirre-Acevedo DC, et al. A three-factor structure of cognitive functioning among unimpaired carriers and non-carriers of autosomal-dominant Alzheimer's disease. *J Alzheimer's Dis*. 2018;65(1): 107-115. https://doi.org/10.3233/JAD-180078.

SUPPORTING INFORMATION

Additional supporting information may be found online in the Supporting Information section at the end of the article.

How to cite this article: Keret O, Staffaroni AM, Ringman JM, et al. Pattern and degree of individual brain atrophy predicts dementia onset in dominantly inherited Alzheimer's disease. *Alzheimer's Dement*. 2021;13:e12197. https://doi.org/10.1002/dad2.12197